Soft Gamma-ray Detector (SGD) onboard the ASTRO-H

Yasushi Fukazawa[a,b] Hiroyasu Tajima[c], Shin Watanabe[d,h], Roger Blandford[e], Katsuhiro Hayashi[d], Atsushi Harayama[d], Jun Kataoka[f], Madoka Kawaharada[d], Motohide Kokubun[d], Philippe Laurent[g], François Lebrun[g], Olivier Limousin[g], Grzegorz M. Madejski[e], Kazuo Makishima[h], Tsunefumi Mizuno[b], Kunishiro Mori[d], Takeshi Nakamori[i], Kazuhiro Nakazawa[h], Hirofumi Noda[j], Hirokazu Odaka[d], Masanori Ohno[a], Masayuki Ohta[d], Shin'ya Saito[d], Goro Sato[f,d], Rie Sato[d], Shin'ichiro Takeda[d], Hiromitsu Takahashi[a], Tadayuki Takahashi[d,h], Yasuyuki Tanaka[b], Yukikatsu Terada[k], Hideki Uchiyama[l], Yasunobu Uchiyama[m], Kazutaka Yamaoka[c], Yoichi Yatsu[n], Daisuke Yonetoku[o], Takayuki Yuasa[j]

[a] Department of Physical Science, Hiroshima University, Higashi-Hiroshima, Hiroshima 739-8526, Japan
[b] Hiroshima Astrophysical Science Center, Hiroshima University, Higashi-Hiroshima, Hiroshima 739-8526, Japan
[c] Solar Terrestrial Environment Laboratory, Nagoya University, Nagoya, Aichi 464-8601, Japan
[d] Institute of Space and Astronautical Science, Japan Aerospace Exploration Agency, Sagamihara, Kanagawa 252-5210, Japan
[e] KIPAC, Stanford University, Stanford, CA 94305, USA
[f] Research Institute for Science and Engineering, Waseda University, Shinjuku-ku, Tokyo, 169-8050, Japan
[g] IRFU / Service d'Astrophysique, CEA Saclay, 91191 Gif-sur-Yvette, Cedex France
[h] Department of Physics, University of Tokyo, Bunkyo-ku, Tokyo 113-0033, Japan
[i] Department of Physics, Faculty of Science, Yamagata University, Kojirakawa, Yamagata 990-8560, Japan
[j] Cosmic Radiation Laboratory, Institute of Physical and Chemical Research (RIKEN) Wako, Saitama 351-0198, Japan
[k] Department of Physics, Saitama University, Saitama, Saitama 338-8570, Japan
[l] Science Education, Faculty of Education, Shizuoka University, Suruga-ku, Shizuoka, 422-8529, Japan
[m] Department of Physics, Rikkyo University, Toshima-ku, Tokyo, 171-8501, Japan
[n] Department of Physics, Tokyo Institute of Technology, Meguro-ku, Tokyo 152-8551, Japan
[o] Department of Physics, Kanazawa University, Kanazawa, Ishikawa 920-1192, Japan

ABSTRACT

The Soft Gamma-ray Detector (SGD) is one of observational instruments onboard the ASTRO-H, and will provide 10 times better sensitivity in 60–600 keV than the past and current observatories. The SGD utilizes similar technologies to the Hard X-ray Imager (HXI) onboard the ASTRO-H. The SGD achieves low background by constraining gamma-ray events within a narrow field-of-view by Compton kinematics, in addition to the BGO active shield. In this paper, we will present the results of various tests using engineering models and also report the flight model production and evaluations.

Keywords: Gamma-ray, Compton telescope, Polarimeter, Silicon, CdTe, Semiconductor detector, BGO

Further author information: (Send correspondence to Y. Fukazawa)
Y. Fukazawa: E-mail: fukazawa@hep01.hepl.hiroshima-u.ac.jp, Telephone: +81 824 24 7380

Space Telescopes and Instrumentation 2014: Ultraviolet to Gamma Ray, edited by Tadayuki Takahashi,
Jan-Willem A. den Herder, Mark Bautz, Proc. of SPIE Vol. 9144, 91442C · © 2014 SPIE
CCC code: 0277-786X/14/$18 · doi: 10.1117/12.2055292

1. INTRODUCTION

The soft gamma-ray detector (SGD) is one of observational instruments onboard the ASTRO-H, the 6th Japanese X-ray observatory. The sensitivity of SGD is about 10 times better than the past and current instruments in 60–600 keV. Together with high-resolution spectroscopy of the SXS and high-sensitive soft and hard X-ray observation of the SXI and HXI, SGD provides us wide-band high-sensitive X-ray observations in 0.4–600 keV. Therefore, we can measure the spectral shape with unprecedented accuracy than ever up to several 100 keV for high energy objects such as black hole binaries, pulsars, active galactic nucleus (AGN), cosmic X-ray background (CXB), and so on. Also, new physics will be opened with 511 keV lines, bremsstrahlung from supernova remnants, and polarization.

Figure 1 shows the cocept of the SGD detector design. Based on technology succession from Suzaku HXD which has achieved the lowest background level than ever in 15–200 keV,[1–3] the SGD utilizes BGO active shields which surround main sensor parts, and fine collimators with a narrow field-of-view of 0.6°(FWHM). Instead of Si PIN diodes and GSO scintillators of HXD, the main sensor part is multi-layer semiconductor Compton camera which we have developed these 13 years[4–20] Compton camera can reduce the background furthermore; incident direction of events with two or more hits in camera is constrained by Compton kinematics and they are rejected if the constrained incident direction is out of a narrow field-of-view. The latter is expected to achieve a lower background level by a factor of ∼100 than HXD. As a result, SGD is expected to achieve about 10 times as good a sensitivity as the past and current instruments in 60–600 keV.

SGD is also a good polarimeter[21, 22] with a large modulation factor of up to 58%, thanks to 3-dim measurements of scattering and absorption positions with stacked pixel sensors. In addition, low background level enables us to measure polarization of celestial objects with down to several 0.01 Crab for the first time in 60–600 keV. Figure 2 shows an expected modulation curve of scattered events for 100 ks observation of sources with 1 Crab or 0.1 Crab flux and 50% polarization degree. Even for 0.1 Crab source, a clear modulation could be obtained.

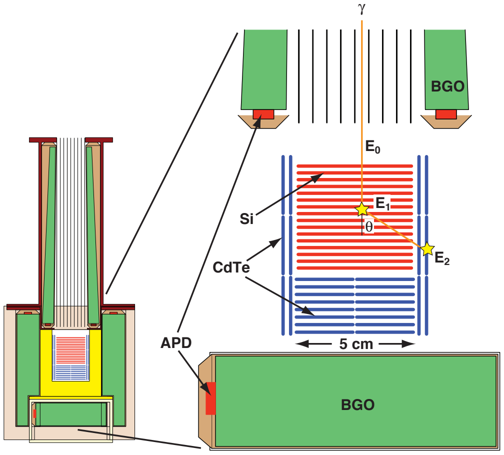

Figure 1. Conceptual drawing of an SGD Compton camera unit.

2. INSTRUMENT DESIGN

Figure 3 shows the SGD electronics block diagram. Design of the SGD electronics system is described in Watanabe et al. (2012)[18] in detail, and here we briefly summarize the design. The SGD electronics system consists of the SGD-S, SGD-AE, SGD-DPU, and SGD-DE. The sensor part SGD-S contains 3 Compton cameras, 25 BGO active shields with Avalanche photo diodes (APD), high voltages, DC/DC converters, charge sensitive amplifiers (CSA) for APD, and they are enclosed in the CFRP housing structure. Also, SGD-S includes a radiator panel, 2×2 heat pipes, heaters, and GFRP interface against the satellite panel. SGD-AE consists of three boards; one is CPMU (Camera Power Management Unit), and the others are APMU (APD Processing and Management Unit), and supplies powers to SGD-S, controls SGD-S besides Compton cameras, and generates

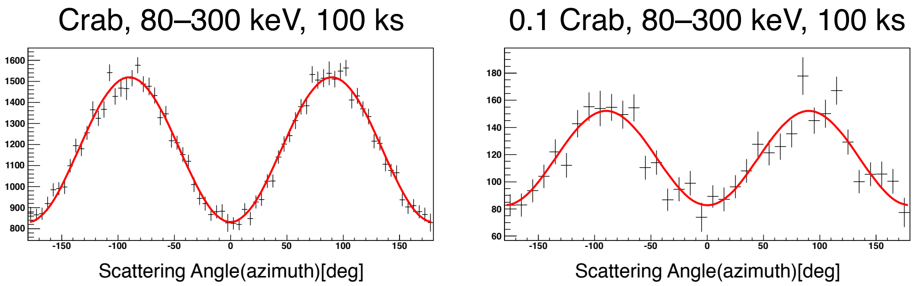

Figure 2. Azimuth angle distribution of Compton scattering from a source with a brightness of 1 Crab and 0.1 Crab in a 100 ks observation. Polarization degrees of 50% are assumed in the both cases.

data of S and AE besides Compton camera. CPMU controls power switches and power supply voltages, and monitors power supply voltages, currents, and temperatures of SGD-S various locations. CPMU also controls the high voltage for Comton Camera in the SGD-S. The APMU receives APD signals from APD CSAs and converts them into digital wave data with flash ADCs, and processed by an FPGA on the APMU to generate several types of anti-coincidence signals for Compton Camwra and create pulse height histograms. Other APMU functions include HK such as control of power switches and power supply voltages, monitor of power supply voltages and temperature. Detailed description of APMU is given in Ohno et al. (2014).[23] SGD-DPU consists of two MIO (Mission I/O) boards and one PSU (Power Supply Unit) board, and supplies powers to AE, sends control signals and formats data of AE and Compton cameras. SGD-DE contains one MDE (Mission Digital Electronics) board and one PSU board, and sends control commands to and receive data from DPU via SpaceWire network interface. Onboard the ASTRO-H, two SGD systems are integrated.

Detailed design of Compton camera of SGD is described in Watanabe et al. (2014).[20] One Compton camera consists of top 32 layers of Si pixel sensors,[24] bottom 8 layers of CdTe pixel sensors,[25, 26] and side 2 layers of CdTe pixel sensors. Si sensors has 16×16 pixels with 0.6 mm thickness, and CdTe has 8×8 pixels with 0.6 mm thickness. Pixel size is 3.2×3.2 mm^2 for both Si and CdTe sensors. Therefore, one bottom or side layer is composed of 2×2 or 2×3 CdTe sensors. A set of 8×8 pixels are read by one ASIC (VATA450.3), and thus there are 208 ASICs in one Compton camera. One ASIC is mounted on one Front-End Card (FEC). Si, CdTe sensors, and FECs are attached to the tray structure, Front-end electronics of the Compton camera consists of four groups of 52 FECs and one ASIC Driver Board (ADB), and one ASIC Control Board (ACB). 8 or 6 FECs (8 or 6 ASICs) are daisy-chained for readout and control. Only power lines and digital lines are required between ADBs and FECs, and all digital signals are differential to minimize the EMI (electro magnetic interference). ASICs are controlled by an FPGA on the ACB. These components are packed in a 12×12×12 cm^3 aluminum box. Such a high-density stacking enables us to obtain a high efficiency of Compton reconstruction of 10–15% around 100 keV.

Figure 4 shows a schematic drawing of SGD-S. The weight and power of SGD-S is 158 kg and ∼24.5W, respectively. The SGD-S is mounted outside of the satellite side-panel and exposed to the space environment, and therefore its thermal design needs special care. Thermal requirement is to keep the temperature of the cold plate attached to Compton camera at -20 ± 5°C and the BGO temperature below -15 ± 5°C with an orbital variation of <3°C. These are necessary to reduce the leakage currents of semiconductor sensors (Si, CdTe, APD) and avoid the gain variation of APD. The concept of thermal design of SGD-S is to transfer the heat, which is generated in the Compton camera and APD CSAs or conducted from the satellite panel, to the radiator attached to the SGD-S as much as possible, and control the temperature via heater support. In this point of view, the main bottom structure holding the Compton camera is directly attached to the heat-pipe and the radiator itself via aluminum structure. The main housing structure is made of CFRP to obtain high rigidity and light weight, and we plated a graphite sheets on its surface to enhance the heat conduction. The SGD-S is mounted to the satellite side-panel via a GFRP base structure to reduce thermal conduction to the CFRP housing. Note that the bottom aluminum structure and the GFRP base structure do not have any direct connection. The APD CSAs are mounted outside the CFRP housing structure via a GFRP arm, and directly connected to the main aluminum bottom structure using the aluminum debris shield.

Heat input from radiation is also non-negligible, such as Infrared (IR) and optical albedo radiation from the earth, and the IR radiation from the satellite structure, including the hot solar paddle located in the opposite side from the radiator. The housing is enclosed by MLIs sheets and additional independent MLI panels are attached at the bottom (to cut sun-lit input) and at the satellite solar panel direction (to cut the IR emission). Thermal design was developed and confirmed by thermal model with the finite element method and some R&D experiments. Thermal structure of Compton camera is designed so that the heat of 4W from ASICs is efficiently sent to the bottom plate which is connected to the heat pipe. Detail description of thermal design of Compton camera is given in Noda et al. (2014).[27]

Mechanical structure of SGD-S must support these complex thermal design and massive BGO scintillators at launch, and also must avoid thermal distortions within SGD-S in orbit. Therefore, the CFRP was employed as the main housing structure. The mechanical structure was developed and confirmed by mechanical model with the finite element method in terms of eigen frequency analysis, quasi-static load, sine vibration, random vibration analysis and acoustic test. The BGO support structures are described in detail in Watanabe et al. (2012).[18] The APD attachment structure also needs some care, especially for thermal distortion between BGO hard surface and APD soft silicone window. We developed a gluing structure as shown in figure 5, where the important point is that not the APD itself but the APD support structure, which pushes APD toward BGO, is glued tightly to the BGO. Issue of mechanical structure of Compton camera is to keep the bonding structure between Si and FEC or between CdTe and readout board. Choice of FEC and bonding material was paid attention to and fine tuning of bonding parameters were performed.

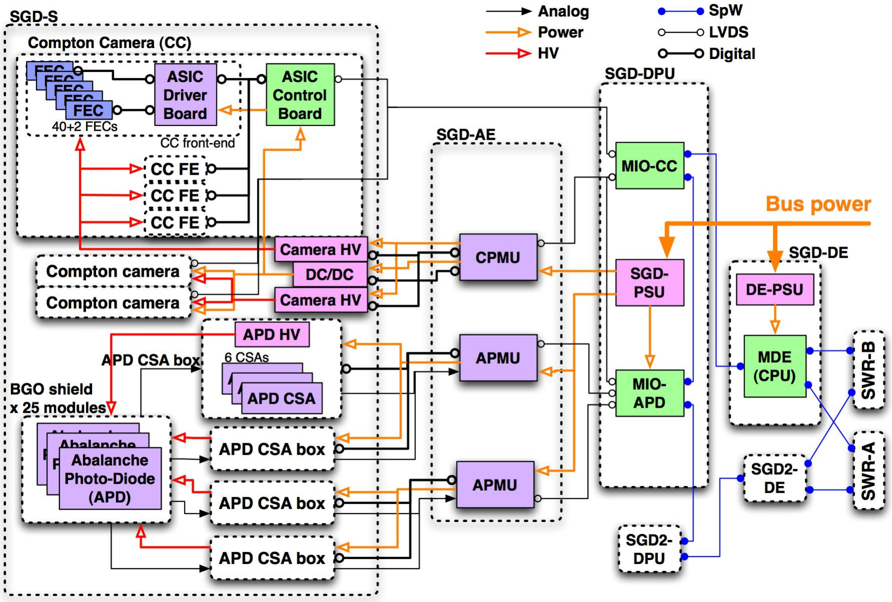

Figure 3. Block diagram of the SGD electronics system.

3. STATUS OF DEVELOPMENT AND FLIGHT MODEL PRODUCTION

In 2012–2013, we performed most of environment tests for SGD-S by using the engineering models whose design is almost the same as those of the flight model. Engineering model of Compton camera contains real Si and CdTe sensors, ASICs and FPGA. Figure 6 shows photos of vibration and acoustic tests of the SGD-S housing and Compton camera. In the test of the housing structure, SGD-S housing is almost the same as the flight model, and 12 BGO active shields and 13 brass dummy weights, as well as one fine collimator were mounted. In the place of Compton camera, there were 3 dummy weights. Radiator and heat pipes are also integrated. The tests were successful and thus mechanical design was validated. Figure 7 shows photos of thermal valance tests of the SGD-S housing and Compton camera in the vacuum. In the former case, we glued heaters in relevant position

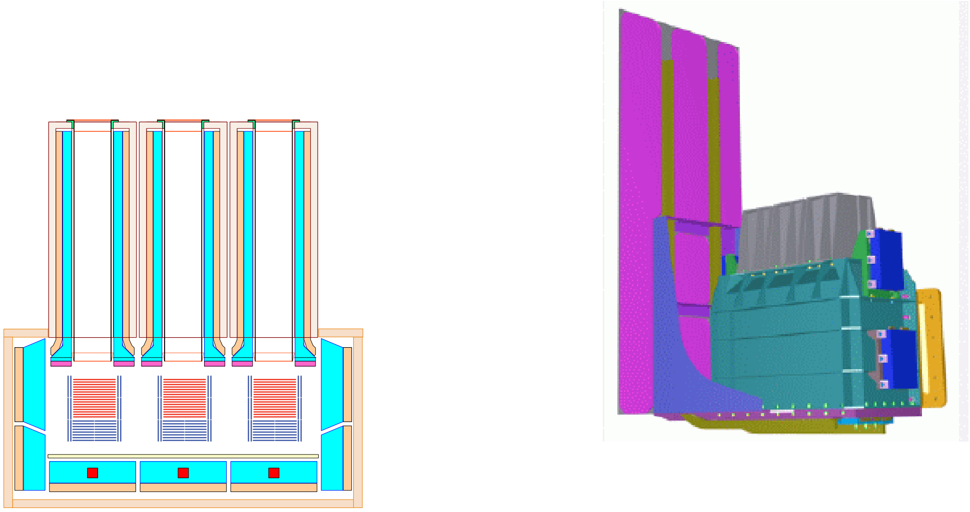

Figure 4. Schematic view of SGD-S sensor parts (left) and housing (right).

to simulate the real sensor parts. The tests were successful and thus thermal design was validated. Detail report on the thermal test of Compton camera was given in Noda et al. (2014).[27]

Also final establishment of electronics design and fine tuning of circuit parameters have been performed in 2012–2014. The most important issue which has not yet established were signal processing of BGO and APD on CSA and APMU. Anti-coincidence signals must be generated so that background rejection is efficiently done with as small dead time as possible. Detailed description on the development and fine tuning is given in Ohno et al. (2014).[23]

Following the success of these tests, production of flight model has been started since 2013. Acceptance tests on leakage current of all APDs are performed before glued to BGOs. Shape-dependence and scatter of BGO light yield were studied in detail by using engineering model. After assembling BGO and APD with support structures, one thermal cycle test from -30°C to 25°C were performed and also BGO light yield was measured. Production has been successful and BGO light yield has been found to be almost the same as expected (figure 8). Fine collimators mounted at the front of Compton camera reduces the CXB and the leakage of gamma-rays from nearby sources. Development, acceptance tests, and alignment procedure of fine collimators are given in detail by Mizuno et al. (2014).[28] R&D studies of Si sensors are reported by Hayashi et al. (2013),[24] and selection of Si sensors for the flight model was based on the measurement results of leakage currents at Hamamatsu Photonics. Acceptance test of CdTe sensors and FECs with ASIC in Compton camera has been performed before mounted as a tray. Acceptance test of trays has been performed before stacked as a Compton camera.

Monte-Carlo simulation of Compton camera is also an important task to develop an efficient algorithm of Compton reconstruction and background rejection, and also construct the response function for data analysis of observational data. Currently, mass model of SGD and other satellite components has been constructed and comparison with data and simulation have been performed by using the data of engineering model of Compton camera, in terms of, for example, reconstructed spectra of two-hits events, count ratios among Si and CdTe sensors, and so on. More sophysticated algorithm of Compton reconstruction for events with more than three hits has been studied. Detail description of Monte-Carlo simulations and those algorithms are given in Ichinohe et al. (2013).[19]

4. EARLY RESULTS OF COMPTON CAMERA AND BGO ACTIVE SHIELD

Since the engineering model of Compton camera was the first fully-stacked one, we performed performance tests by using this camera. Detail description of performance tests is reported by Watanabe et al. (2014),[20] and thus

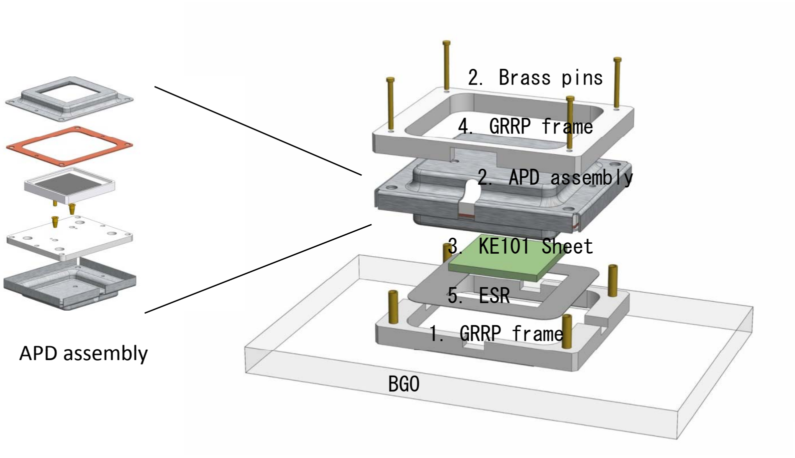

Figure 5. BGO + APD gluing structure.

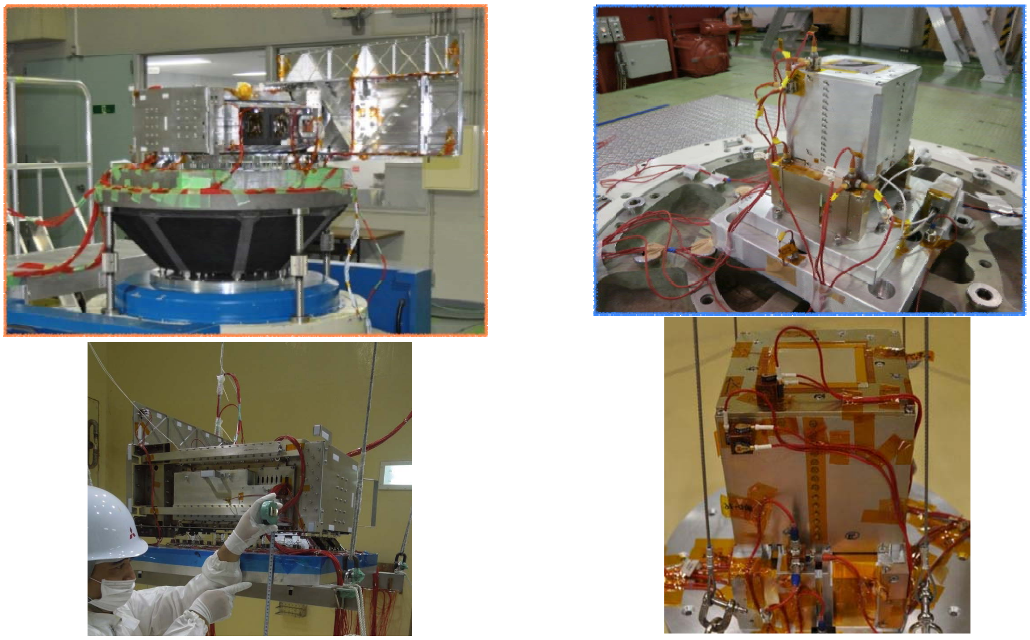

Figure 6. Photos of vibration tests (top) and acoustic tests (bottom) of engineering models of SGD-S housing (left) and Compton camera (right).

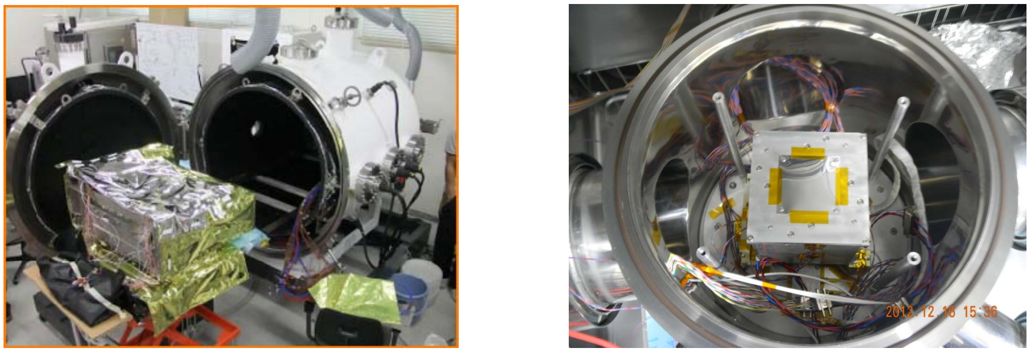

Figure 7. Photos of thermal balance tests in the vacuum of engineering models of SGD-S housing (left) and Compton camera (right).

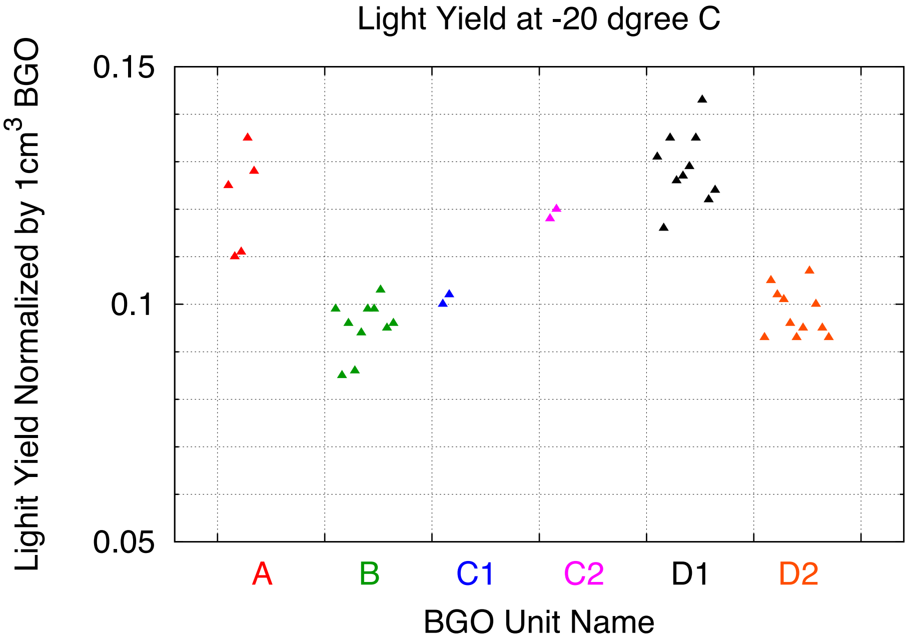

Figure 8. BGO light yield after assembling BGO, APD, and support structures. Light yield is normalized by the light yield of 1 × 1 × 1 cm^3 BGO. D1 and D2 are BGOs located at the top, while others are BGO located at the bottom.

here we briefly report it. Figure 9 shows a reconstructed spectrum of Compton-scattered events with two or three hits at Si and CdTe sensors. Photo peak of 662 keV ^{137}Cs gamma-ray is clearly reconstructed with an energy resolution of 10.5 keV (FWHM) for tw-hits events.

One engineering model and two flight models of Compton camera, and 25 BGO active shields are integrated in the flight model housing in 2014 spring for end-to-end test, which was for the first time performed with the electronics of pre-flight or flight models (figure 10). Since the test has been done only at room temperature, performance of Compton camera was not evaluated but noise performance is as good as expected and data readout were almost successful. Cosmic ray events were successfully recorded by the Compton camera as linear hits as shown in figure 11. 11 of 25 BGO active shields were read out in this test and their spectra are shown in figure 12. In this case, only background events were measured and the spectrum was as expected with threshold of ~700 keV at room temperature and several strong background lines at 1.46 MeV and 2–3 MeV are seen, together with muon events above 3 MeV. Using this sensor, we for the first time took the anti-coincidence between Compton camera and BGO active shields. In order to check that anti-coincidence signals are generated as expected, we utilized cosmic-ray events which are recorded as linear hits in Comton camera. Figure 13 shows a histogram of the number of hits for linear-hits events with or without anti-coincidence flags. About 50% of such linear events are confirmed to coincide with BGO anti-coincidence signals. This fraction is reasonable since 11 BGO active shields read out in this test covers the Compton cameras with a solid angle of about 50%. Therefore, processing of anti-coincidence signals is working well.

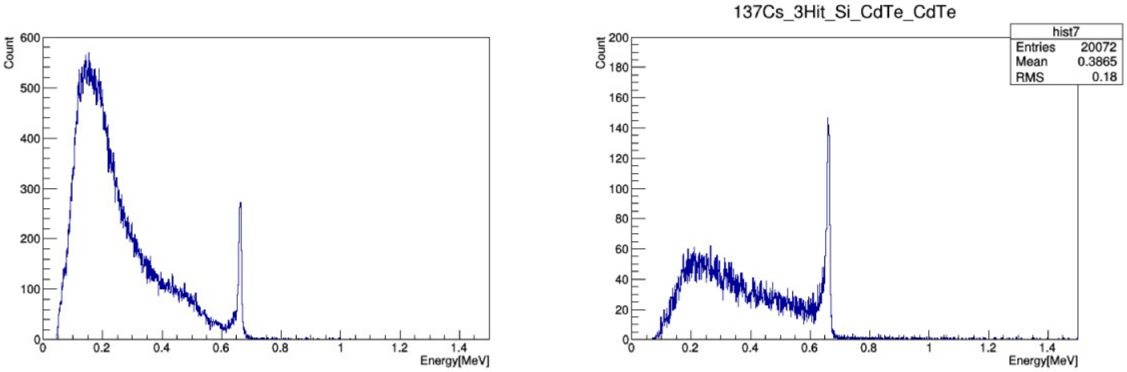

Figure 9. Compton-reconstructed Spectra of ^{137}Cs gamma-ray sources for two-hits (left) and three-hits (right) events.

5. SUMMARY AND TOWARD THE LAUNCH

The design of SGD has been almost completed, and currently production of flight model continues to be finished in 2014. First of all, we plan performance test of Compton camera at operation temperature at -20°C. After that, all environment tests (vibration, shock, acoustic, thermal balance in the vacuum, calibration, and EMI) will be planned before delivery to the ASTRO-H at the end of 2014.

REFERENCES

[1] Takahashi, T. et al., "Hard x-ray detector (hxd) on board suzaku," *PASJ* **59**, S35 (2007).

[2] Takahashi, T. et al., "In-orbit performance of the hard x-ray detector (hxd) on board suzaku," *PASJ* **59**, S53 (2007).

[3] Fukazawa, Y. et al., "Modeling and reproducibility of Suzaku HXD PIN/GSO background," *Pub. of Astro. Soc. of Japan* **61**, S17 (2009).

[4] Takahashi, T., Kamae, T., and Makishima, K., "Future hard X-ray and gamma-ray observations," *Proc. SPIE* **251**, 210–213 (2002).

[5] Takahashi, T., Nakazawa, K., Kamae, T., Tajima, H., Fukazawa, Y., Nomachi, M., and Kokubun, M., "High resolution CdTe detectors for the next generation multi-Compton gamma-ray telescope," in [*X-ray and Gamma-ray Telescopes and Instruments for Astronomy, SPIE*], Truemper, J. E. and Tananbaum, H. D., eds., **4851**, 1228–1235 (2002).

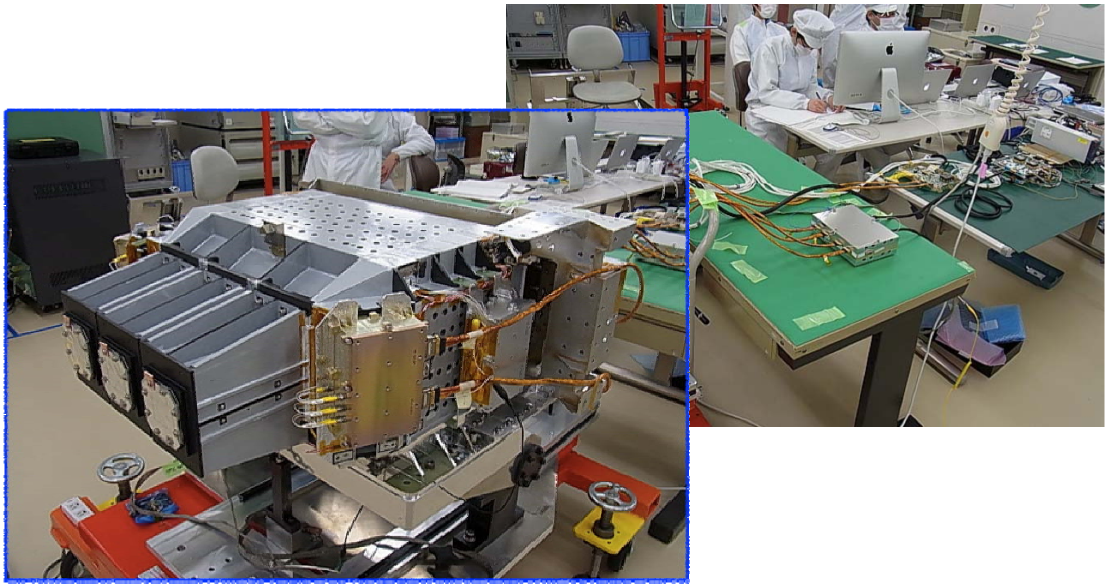

Figure 10. Photo of end-to-end test with SGD-S (most parts are flight models) and electronics (pre flight or flight models).

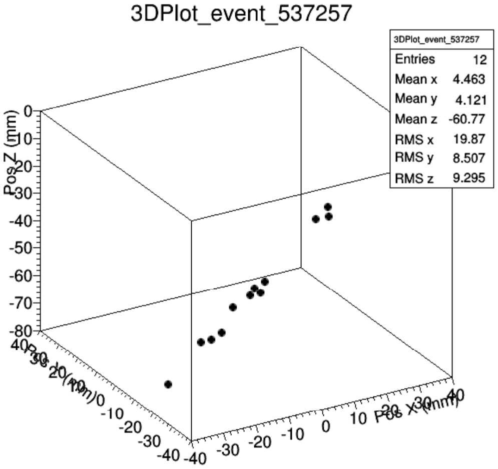

Figure 11. Example of linear-hits events due to cosmic rays.

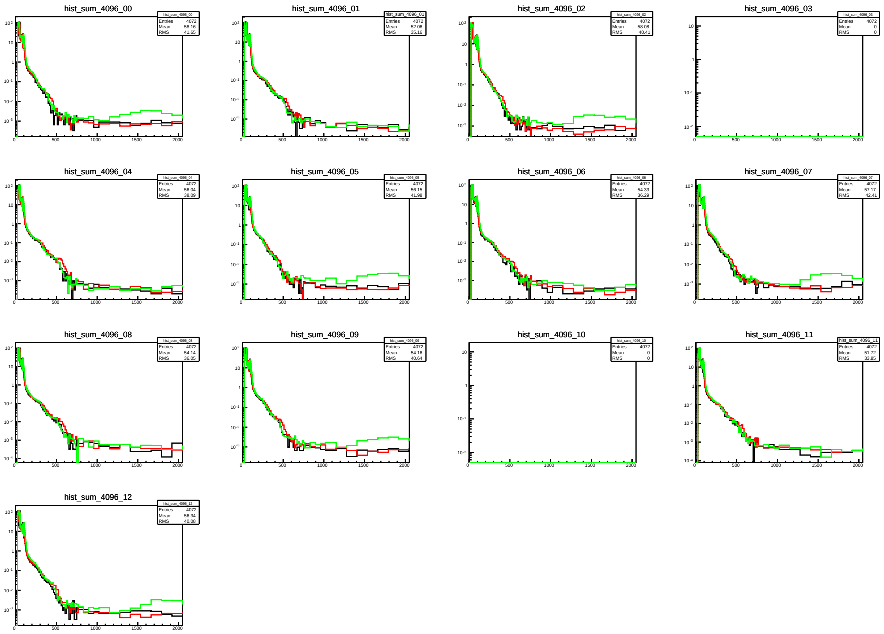

Figure 12. Background spectra of 11 BGO active shields read out in end-to-end test. Colors represent different experimental days.

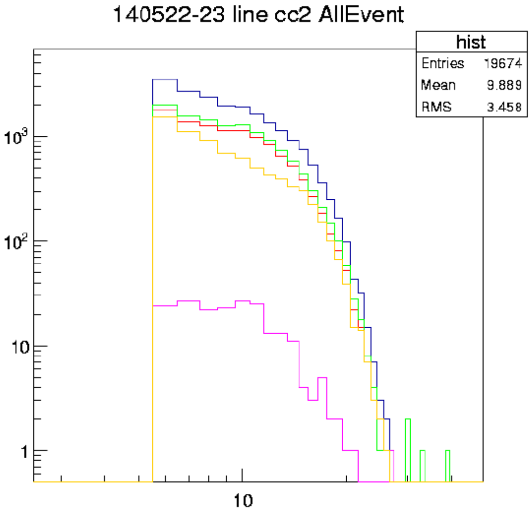

Figure 13. Histogram of the number of hits in one event for linear-hits events (likely cosmic rays). Green, red, cyan are events with anti-coincidence flags of HITPAT, FastBGO, and UD, respectively. Yellow is events without any anti-coincidence flags.

[6] Tajima, H., "Gamma-ray polarimetry," *Nucl. Instrum. Methods A* **511**, 287–290 (2003).

[7] Takahashi, T., Makishima, K., Fukazawa, F., Kokubun, M., Nakazawa, K., Nomachi, M., Tajima, H., Tashiro, M., and Terada, Y., "Hard X-ray and Gamma-ray detectors for the NeXT mission," *New Astro. Rev.* **48**, 309–313 (2004).

[8] Mitani, T., Tanaka, T., Nakazawa, K., Takahashi, T., Takashima, T., Tajima, H., h. Nakamura, Nomachi, M., Nakamoto, T., and Fukazawa, Y., "Prototype of Compton camera using high resolution Si/CdTe detectors," *IEEE Trans. Nucl. Sci.* (2004).

[9] Takahashi, T., Awaki, A., Dotani, T., Fukazawa, Y., Hayashida, K., Kamae, T., Kataoka, J., Kawai, N., et al., "Wide-band X-ray imager (WXI) and soft gamma-ray detector (SGD) for the NeXT mission," *Proc. SPIE* **5488**, 549–560 (2004).

[10] Tanaka, T., Mitani, T., Nakazawa, K., Oonuki, K., Sato, G., Takahashi, T., Tamura, K., Watanabe, S., Tajima, H., Nakamura, H., Nomachi, M., Nakamoto, T., and Fukazawa, Y., "Development of Si/CdTe semiconductor Compton telescope," in [*High Energy Detectors in Astronomy*], *SPIE* **5501**, 229–240 (2004).

[11] Watanabe, S., Tanaka, T., Nakazawa, K., Mitani, T., Kousuke, K., Takahashi, T., Takashima, T., Tajima, H., Fukazawa, Y., Nomachi, M., Kubo, S., Onishi, M., and Kuroda, Y., "Si/CdTe semiconductor Compton camera," in [*Proceedings of IEEE Nuclear Science Symposium*], (2004).

[12] Takahashi, T., Makishima, K., Fukazawa, Y., Kokubun, M., Nakazawa, K., Nomachi, M., Tajima, H., Tashiro, M., and Terada, Y., "Hard x-ray and γ-ray detectors for the next mission," *New Astronomy Reviews* **48**, 269–273 (2004).

[13] Watanabe, S., Tanaka, T., Nakazawa, K., Mitani, T., Oonuki, K., Takahashi, T., Takashima, T., Tajima, H., Fukazawa, Y., Nomachi, M., Kubo, S., Onishi, M., and Kuroda, Y., "A Si/CdTe semiconductor Compton camera," *IEEE Trans. Nucl. Sci.* **52**, 2045–2051 (2005).

[14] Odaka, H., Takeda, S., Watanabe, S., Ishikawa, S., Ushio, M., Tanaka, T., Nakazawa, K., Takahashi, T., Tajima, H., and Fukazawa, Y., "Performance study of Si/CdTe semiconductor Compton telescopes with monte carlo simulation," *Nucl. Instrum. Methods A* **579**, 878–885 (2007).

[15] Takeda, S., Aono, H., Okuyama, S., n. Ishikawa, S., Odaka, H., Watanabe, S., Kokubun, M., Takahashi, T., Nakazawa, K., Tajima, H., and Kawachi, N., "Experimental results of the gamma-ray imaging capability with a Si/CdTe semiconductor Compton camera," *IEEE Trans. Nucl. Sci.* **56**, 783–790 (2009).

[16] Tajima, H. et al., "Soft gamma-ray detector for the ASTRO-H mission," *Proc. SPIE* **7732**, 73216–773216–17 (2010).

[17] Takeda, S., Odaka, H., Ishikawa, S., Watanabe, S., Aono, H., Takahashi, T., Kanayama, Y., Hiromura, M., and Enomoto, S., "Demonstration of in-vivo multi-probe tracker based on a Si/CdTe semiconductor Compton camera," *IEEE Trans. Nucl. Sci.* **59**, 70–76 (2012).

[18] Watanabe, S. et al., "Soft gamma-ray detector for the ASTRO-H mission," *Proc. SPIE* **8443**, 844326 (2012).

[19] Ichinohe, Y. et al., "Study of event reconstruction algorithm for a large-scale si/cdte multilayer compton camera," *Proc. Nuclear Science Symposium and Medical Imaging Conference (NSS/MIC)* (2013).

[20] Watanabe, S. et al., "The si/cdte semiconductor compton camera of the astro-h soft gamma-ray detector," *To appear in Nucl. Instrum. Methods A* (2014).

[21] Tajima, H., Madejski, G., Mitani, T., Tanaka, T., Nakamura, H., Nakazawa, K., Takahashi, T., Fukazawa, Y., Kamae, T., Kokubun, M., Marlow, D., Nomachi, M., and Silva, E. C., "Gamma-ray polarimetry with Compton telescope," in [*UV and Gamma-Ray Space Telescope Systems*], *SPIE* **5488**, 561–571 (2004).

[22] Takeda, S., Odaka, H., Katsuta, J., Ishikawa, S., Sugimoto, S., Koseki, Y., Watanabe, S., Sato, G., Kokubun, M., Takahashi, T., Nakazawa, K., Fukazawa, Y., Tajima, H., and Toyokawa, H., "Polarimetric performance of Si/CdTe semiconductor Compton camera," *Nucl. Instrum. Methods A* **622**, 619–627 (2010).

[23] Ohno, M. et al., "Development and verification of signal processing of bgo active shield onboard astro-h," *Proc. SPIE* **9144**, 9144–214 (2014).

[24] Hayashi, K., Park, I., Dotsu, K., Ueno, I., Nishino, S., Matsuoka, M., Yasuda, H., Fukazawa, Y., Ohsugi, T., Mizuno, T., Takahashi, H., Ohno, M., Endo, S., Tanaka, T., Tajima, H., Kokubun, M., Watanabe, S., Takahashi, T., Nakazawa, K., Uchihori, Y., and Kitamura, H., "Radiation effect on the silicon semiconductor detectors for the astro-h mission," *Nucl. Instrum. Methods A* **699**, 225–229 (2013).

[25] Takahashi, T., Nakazawa, K., Watanabe, S., Sato, G., Mitani, T., Tanaka, T., Onuki, K., Tamura, K., Tajima, H., Nomachi, M., Fukazawa, Y., and Kokubun, M., "Application of CdTe for the NeXT mission," *To appear in Nucl. Instrum. Methods A* (2004).

[26] Watanabe, S., Ishikawa, S., Aono, H., Takeda, S., Odaka, H., Kokubun, M., Takahashi, T., Nakazawa, K., Tajima, H., Onishi, M., and Kuroda, Y., "High energy resolution hard X-ray and gamma-ray imagers using CdTe diode devices," *IEEE Trans. Nucl. Sci.* **56**, 777–782 (2009).

[27] Noda, H. et al., "Thermal design of the hard x-ray imager and soft gamma-ray detector onboard astro-h," *Proc. SPIE* **9144**, 9144–212 (2014).

[28] Mizuno, T. et al., "Developement and calibration of fine collimators for the soft gamma-ray detector oboard astro-h," *Proc. SPIE* **9144**, 9144–213 (2014).